Palestine Journal of Mathematics

Vol. 10(Special Issue I)(2021) , 59–68

Combined Effect of Rough Surface with MHD on Porous Conical Bearing with Conducting Couple-Stress Fluid

Hanumagowda B N, Salma A and Swapna S Nair

Communicated by V. Lokesha

MSC 2010 Classifications: Primary 76W99, 76D08, 76A05; Secondary 376D08,74DXX,76E25.

Keywords and phrases: MHD, Couple stress fluid, Surface roughness, Porous medium, Conical bearings

Abstract In this article, the combined effect of magnetic field and surface roughness on the squeeze film lubrication between porous conical bearing lubricated with couple stress fluid is presented. Based on Christensen's stochastic theory for rough surface, the modified Reynolds equation is derived and the expression for mean fluid pressure, mean load carrying capacity and squeeze film time was examined on the roughness pattern. The results are plotted graphically for various dimensionless parameter such as Hartmann number, couple stress parameter, permeability parameter and roughness parameter. It was observed that pressure, load carrying capacity and squeeze film time increases with the effect of magnetic field and couple stress in the presence of surface roughness compared to non-magnetic case and Newtonian case, whereas these parameters decrease in the presence of surface roughness as half-cone angle increases.

1 Introduction

The impact of MHD on the squeeze film lubrication is very promising since magnetic field has significant applications in the industry. Maki and Kuzma[1] performed experimental and theoretical research in MHD hydrostatic bearings and found that use of electrically conducting lubricant with applied magnetic field gives effective performance of squeeze film bearings. Naduvinamani et.al [2] analyzed the impact of couple stress and MHD on the characteristics of squeeze-film in circular stepped plates. In recent year, many research scholars are showing considerable interest in hydrodynamic lubrication theory for roughness, as all the surfaces of bearing are rough to some level. Numerous methodologies have been put forward in the literature to understand the impact of rough surface on bearings. Christensen[4] was the first to study about the rough surfaces in hydrodynamic lubrication of solid bearings who investigated a stochastic model. Since then many researchers[5-8] have embraced this concept and applied this approach to study the effect of rough bearing surfaces to deploy the stochastic model.

Kudenatti and Bujurke [3] researched on the consequences of roughness across rectangular plates containing electrically conducting fluid, having a rough surface on the upper plate. The classical Reynolds equation was generated and showed that the impact of rough surface and MHD increases the pressure distribution and load supporting capacity.

Tzeng and Saibel [9-10] used stochastic concepts to understand the surface roughness effects in slider bearings and in short journal bearing. Many investigators [11-15] used Stokes couplestress fluid theory for analyzing the performance of different types of bearing with surface roughness Hanumagowda et.al [16] explained the impact of CSF between conical bearing with MHD and surface roughness and noticed that the attributes of squeeze film lubrication performs better in case of Azimuthal pattern than in Radial roughness pattern. Prakash and Tiwari [17] studied the impact of rough surface to understand the characteristics of squeeze-film between porous rectangular plates. Later Ramesh et.al [18] numerically analyzed the effect of magnetic field and surface roughness on rough and porous rectangular plates. They found that pressure and load carrying capacity is more dominant for increasing Hartmann-number and roughness parameter values and decreases for increasing permeability parameter. So far, we have not seen the joined impact of MHD, CSF and rough surface on the performance of squeeze film across porous conical bearing. In this chapter we study the joined impact of couple-stress, roughness

on porous conical bearing with transverse magnetic field.

2 Mathematical formulation and theoretical Solution

A squeezing flow of couple stress fluid between rough $(z = 0)$ porous conical bearing is presented in figure 1. A uniform magnetic field $\mathbf{B}_0$vertically from the bottom of the conical bearing is applied.

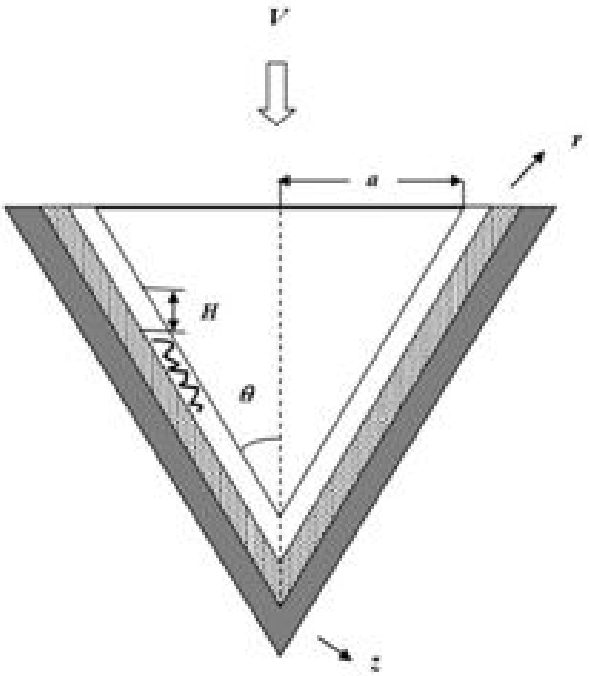

Figure 1. Geometrical representation of Porous Conical plates

The basic equation for MHD couple stress fluid is given by:

$$\frac{\partial^2 u}{\partial z^2} - \frac{\eta}{\mu}\frac{\partial^4 u}{\partial z^4} - \frac{\mu {M_0}^2}{\mu {h_0}^2}u = \frac{1}{\mu}\frac{\partial p}{\partial r} \tag{2.1}$$

$$\frac{\partial p}{\partial z} = 0 \tag{2.2}$$

$$\frac{1}{r}\frac{\partial}{\partial r}(ru) + \frac{\partial w}{\partial z} = 0 \tag{2.3}$$

Boundary Conditions are:

At lower surface $z = 0$

$$u = 0 \qquad w = w^* \tag{2.4}$$

At Upper surface $z = h\sin\theta$

$$u = 0 \qquad w = sin\theta {}^{dh}/_{dt} \tag{2.5}$$

Solving equation (2.1) and using above boundary conditions we get

$$u = -\frac{1}{(A^2 - B^2)}\frac{h_0^2}{\mu M_0^2}\frac{\partial p}{\partial r}\left\{\left(\frac{B^2 Cosh\frac{A(2y-hSin\theta)}{2l}}{Cosh\frac{AhSin\theta}{2l}} - \frac{A^2 Cosh\frac{B(2y-hSin\theta)}{2l}}{Cosh\frac{BhSin\theta}{2l}}\right) + (A^2 - B^2)\right\} \tag{2.6}$$

Substituting above equation in (2.3) and integrating across film thickness h we get a modified Reynolds equation

$$\frac{1}{r}\frac{\partial}{\partial r}\left\{rg(h,\theta,l,M_0)\frac{\partial p}{\partial r}\right\} = -^{dh}/_{dt}sin\theta + w|_0 \tag{2.7}$$

Where
$g(h,\theta,l,M_0) = \frac{h_0^2}{\mu M_0^2}\left\{\frac{2l}{A^2-B^2}\left(\frac{B^2}{A}\tanh\frac{AhSin\theta}{2l} - \frac{A^2}{B}\tanh\frac{BhSin\theta}{2l}\right) + hSin\theta\right\}$
Porous conditions:

$$u^* = \frac{-k}{\mu\left[1-\phi+\frac{kM^2}{mh_0^2}\right]}\frac{\partial p^*}{\partial r} \tag{2.8}$$

$$w^* = \frac{-k}{\mu\left[1-\phi\right]}\frac{\partial p^*}{\partial z} \tag{2.9}$$

$$\frac{1}{r}\frac{\partial}{\partial r}(ru^*) + \frac{\partial w^*}{\partial z} = 0 \tag{2.10}$$

Where , $\mu \rightarrow$ viscosity coefficient $\eta \rightarrow$ material constant characterizing couple stress,$\phi = (\eta/\mu)/k \rightarrow$ ratio of microstructure size to pore size,$m \rightarrow$ porosity, $k \rightarrow$ permeability of porous material.

The component of velocity in the z-direction is continuous at the interface between the plate and the film so that

$$w_0 = -\left[\frac{dh}{dt} + \frac{k}{\mu\left[1-\phi\right]}\left(\frac{\partial p^*}{\partial z}\right)_{z=0}\right] \tag{2.11}$$

From (2.7)

$$\frac{1}{r\mu}\frac{\partial}{\partial r}\left\{rf(h,\theta,l,M_0)\frac{\partial p}{\partial r}\right\} = \frac{dh}{dt} + \frac{k}{\mu\left[1-\phi\right]}\left(\frac{\partial p^*}{\partial z}\right)_{z=0}\sin\theta \tag{2.12}$$

The pressure in the porous region is

$$\frac{1}{r}\frac{\partial}{\partial r}\left(r\frac{\partial p^*}{\partial r}\right) + \left[\frac{D}{1-\phi}\right]\frac{\partial p^*}{\partial z^2} = 0 \quad , \quad \text{where} \quad D = \left[1-\phi+\frac{kM^2}{mh_0^2}\right]$$

Let us integrate above equation wrt z over porous layer thickness δ

$$\frac{\partial p^*}{\partial r} = 0 \; at \; z = -\delta$$

we obtain

$$\left[\frac{\partial p^*}{\partial z}\right]_{z=0} = -\left[\frac{1-\phi}{D}\right]\int_{-\delta}^{0}\frac{1}{r}\frac{\partial}{\partial r}\left(r\frac{\partial p^*}{\partial r}\right)\,dz$$

Assuming that the thickness δ of porous layer is very small & using the pressure continuity condition $p = p^*$ at porous interface $z = 0$ we get

$$\left[\frac{\partial p^*}{\partial z}\right]_{z=0} = -\delta\left[\frac{1-\phi}{D}\right]\;\frac{1}{r}\frac{\partial}{\partial r}\left(r\frac{\partial p}{\partial r}\right)$$

sub in eq (2.12) we get

$$\frac{1}{r}\frac{\partial}{\partial r}\left\{\left(g(h,\theta,l,M_0) + \frac{\delta k\sin\theta}{D}\right)r\frac{\partial p}{\partial r}\right\} = -\mu V\sin\theta \tag{2.13}$$

Equation (2.13) is the modified Reynold's equation.
Christensen's theory[4] for roughness considers two parts of the thickness H ,

$$H = h + h_s(r,\theta,\xi) \tag{2.14}$$

Where h is the smooth part, h_s represents the stochastic film thickness and ξ represents index parameter for exact roughness pattern .
Taking the expected values of (2.13) we get Reynolds equation as

$$\frac{1}{r}\frac{\partial}{\partial r}\left\{E(g(h,\theta,l,M_0))r\frac{\partial E(p)}{\partial r}\right\} = -\mu V Sin\theta \tag{2.15}$$

Where E is the expected value, defined as

$$E(\bullet) = \int_{-\infty}^{\infty} (\bullet)p_1(h_s)dhs \tag{2.16}$$

Here p_1 is probability density-function and Christensen[4] stochastic model gives:

$$p_1(h_s) = \begin{cases} \frac{35}{32n^7}(n^2 - {h_s}^2)^3, -n < h_s < n \\ 0, \quad elsewhere \end{cases}$$

Where $\sigma = n/3$ represents standard deviation
We take into consideration, two types of one-dimensional roughness patterns
Radial Roughness Pattern. The one-dimensional radial roughness structure is in form of ridge, valley and long that passes in r-direction. The film thickness and generalized Reynolds equation for radial structure is

$$H = h(t) + h_s(\theta,\xi)$$

$$\frac{1}{r}\frac{\partial}{\partial r}r\left\{\frac{\partial E(p)}{\partial r}\left(E(g(h,\theta,l,M_0)) + \frac{\delta k\sin\theta}{D}\right)\right\} = -\mu V\sin\theta \tag{2.17}$$

Azimuthal Roughness Pattern. The one-dimensional azimuthal roughness structure is in form of ridge, valley and circular that passes in θ-direction .The film thickness and generalized Reynolds equation for azimuthal pattern is

$$H = h(t) + h_s(r,\xi)$$

$$\frac{1}{r}\frac{\partial}{\partial r}\left[r\frac{\partial E(P)}{\partial r}\frac{1}{\left\{E(\frac{1}{g(h,\theta,l,M_0)}) + \frac{\delta k\sin\theta}{D}\right\}}\right] = -\mu V Sin\theta \tag{2.18}$$

Equation (2.17) and (2.18) together can be expressed as

$$\frac{1}{r}\frac{\partial}{\partial r}\left\{r\frac{\partial E(p)}{\partial r}J(h,\theta,l,M_0,n) + \frac{\delta k\sin\theta}{D}\right\} = -\mu V Sin\theta \tag{2.19}$$

Where,

$$J(h,\theta,l,M_0,n) = \begin{cases} E(g(h,\theta,l,M_0)), & for\, radial \\ E\left(\frac{1}{g(h,\theta,l,M_0)}\right)^{-1}, & for\, azimuthal \end{cases}$$

Where,

$$E(g(h,\theta,l,M_0) = \frac{35}{32n^7}\int_{-n}^{n} g(h,\theta,l,M_0)(n^2 - {h_s}^2)^3 dh_s$$

$$E\left\{\frac{1}{g(h,\theta,l,M_0)}\right\} = \frac{35}{32n^7}\int_{-n}^{n}\frac{(n^2 - {h_s}^2)^3}{g(h,\theta,l,M_0)}dh_s$$

The non-dimensionless parameters are given as

$$r^* = \frac{r}{aCo\sec\theta}, l^* = \frac{2l}{h_0}, h^* = \frac{h}{h_0}, P^* = -\frac{E(P)h_0^3}{\mu a^2(dh/dt\ )Co\sec\theta}, C = \frac{n}{h_0}$$

$$= \frac{k\delta\sin\theta}{h_0^3}, D_1 = \left[1 - \phi + \frac{\psi M^2}{m\delta^*}\right]$$

Equation (2.19) reduces to

$$\frac{1}{r^*}\frac{\partial}{\partial r^*}\left\{r^*\frac{\partial P^*}{\partial r^*}J(h^*, \theta, l^*, M_0, \psi, C)\right\} = -1 \tag{2.20}$$

$$\frac{\partial P^*}{\partial r^*} = 0 \qquad \text{at} \qquad r^* = 0 \qquad \text{and} \qquad p^* = 0 \qquad \text{at} \qquad r^* = 1 \tag{2.21}$$

On Integrating (2.20) using the above condition we get film pressure P^* as

$$P^* = \frac{1 - r^{*2}}{4J(h^*, \theta, l^*, M_0, \psi, C)} \tag{2.22}$$

Integrating the above pressure we obtain non-dimensional load carrying capacity

$$W^* = \frac{E(W){h_0}^3}{\mu a^4\pi(-dh/dt\ )Co\text{sec}^2\theta} = \frac{1}{8J(h^*, \theta, l^*, M_0, \psi, C)} \tag{2.23}$$

Integrating above load expression with initial condition

$$h^*(t^* = 0) = 1$$

We obtain non-dimensionless squeezing time as.

$$T^* = \frac{E(W){h_0}^2}{\mu a^4\pi\cos ec^2\theta} = \int_{h^*{}_1}^{1}\left\{\frac{1}{8J(h^*, \theta, l^*, M_0, \psi, C)}\right\}dh^* \tag{2.24}$$

3 Results and discussion

In the present article, the combined impact of MHD, CSF and roughness on the performance of squeeze-film across porous conical bearing using Christensen stochastic theory and Stokes couple stress theory is studied. The result are discussed for various non-dimensional factors, such as Hartmann number M_0, half-cone angle θ ,couple-stress parameter l^*, parameter of permeability ψ and parameter of roughness C. For graphical and numerical interpretation on the above parameter, following ranges are assumed: $l^* = 0, 0.2, 0.4, C = 0, 0.2, 0.4, M_0 = 0, 2, 4, \psi = 0, 0.01, 0.1, \theta = \frac{\pi}{4}, \frac{\pi}{3}, \frac{\pi}{2}$.

3.1 Dimensionless Pressure:

Deviation of dimensionless P^* versus r^* for distinct C values with $M_0 = 2, l^* = 0.3, \theta = \pi/3$ for $\psi = 0.001$ is shown in figure 2. It is observe that for larger C values, P^* inclines in azimuthal structure whereas pressure declines in radial pattern. Figure 3 represents P^* with respect to r^* as a function of Hartmann number M_0 for permeability parameter $\psi = 0.001$. It is notice that pressure raises with the effect of magnetic field for radial and azimuthal structure. Figure.4 presents the impacts of parameter l^* with respect to r^* and it is noted that the effect of l^* is to enhance the P^*. The profile of pressure P^* versus r^* for distinct values with $C = 0.2, M_0 = 2, l^* = 0.$ for permeability parameter $\psi = 0.001$ is displayed in figure 5 and noticed that for both the roughness structure, pressure declines as increases. Figure 6 elaborates, the pressure P^* with respect to r^* as a function of permeability parameter for both the roughness structure and implies that permeability parameter decreases P^*

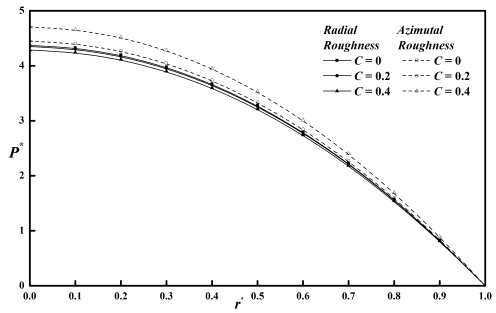

Figure 2: Variation of non-dimensional P^* with r^* for different values of C with $M_0 = 2$, $l^* = 0.3$, $\theta = \pi/3$, $h = 1.2$, $\psi = 0.001$, $m = 0.6$, $\delta = 0.01$, $\phi = 0.2$.

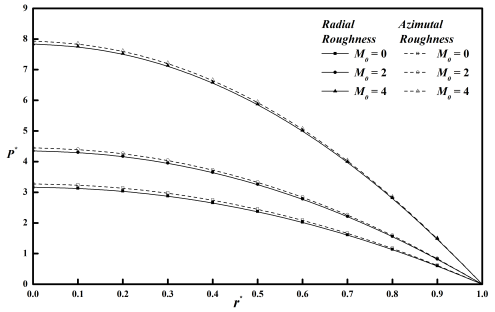

Figure 3: Variation of non-dimensional P^* with r^* for different values of M_0 with $C = 0.2$, $l^* = 0.3$, $\theta = \pi/3$, $h = 1.2$, $\psi = 0.001$, $m = 0.6$, $\delta = 0.01$, $\phi = 0.2$.

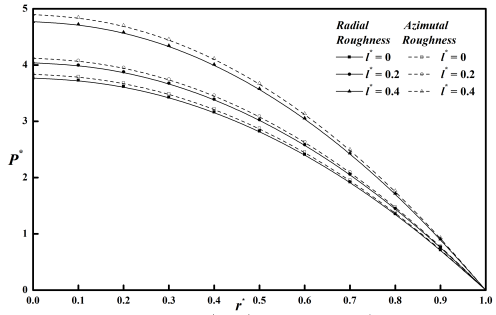

Figure 4: Variation of non-dimensional P^* with r^* for different values of l^* with $M_0 = 2$, $C = 0.2$, $\theta = \pi/3$, $h = 1.2$, $\psi = 0.001$, $m = 0.6$, $\delta = 0.01$, $\phi = 0.2$.

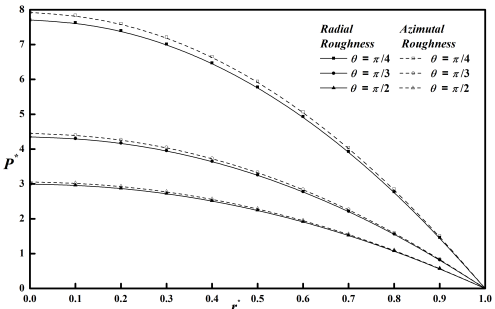

Figure 5: Variation of non-dimensional P^* with r^* for different values of θ with $M_0 = 2$, $C = 0.2$, $l^* = 0.3$, $h = 1.2$, $\psi = 0.001$, $m = 0.6$, $\delta = 0.01$, $\phi = 0.2$.

3.2 Dimensionless Load supporting Capacity:

Figure 7 shows the variation in load W^* against h^* as a function of parameter C with $M_0 = 2, l^* = 0.3, \theta = \pi/3, \psi = 0.001$. The figure implies that as parameter C increases, W^* increases in azimuthal pattern compared to radial structure. In Figure 8, it is notice that for the higher Hartmann number M_0 values, the load W^* increases for both the roughness pattern for permeability parameter $\psi = 0.001$. The graph W^* against h^* with parameter l^* as a function is shown in figure 9 and observed that the impact of couplestress parameter is to increase the load W^* for both radial and azimuthal roughness pattern. The variation in load carrying capacity with h^* for distinct values with $C = 0.2, M_0 = 2, l^* = 0.3$ and $\psi = 0.001$ is projected in figure 10. It is notice that as θ values increases ,the load carrying capacity reduces for both the roughness pattern. Variation in load-carrying capacity for different ψ values with $M_0 = 2, l^* = 0.3, \theta = \pi/3$ and $C = 0.2$ is shown in figure 11. which implies that for both roughness structure W^* reduces for greater permeability parameter ψ values

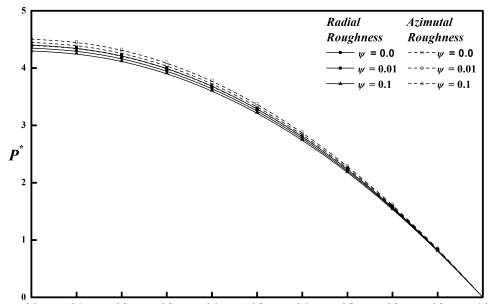

Figure 6: Variation of non-dimensional P^* with r^* for different values of ψ with $M_0 = 2$, $C = 0.2$, $l^* = 0.3$, $h = 1.2$, $\theta = \pi/3$, $m = 0.6$, $\delta = 0.01$, $\phi = 0.2$.

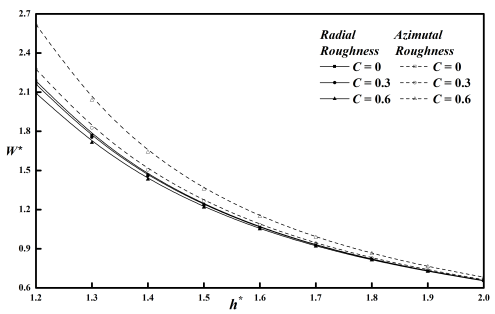

Figure 7: Variation of non-dimensional W^* with h^* for different values of C with $M_0 = 2$, $l^* = 0.3$, $\theta = \pi/3$, $\psi = 0.001$, $m = 0.6$, $\delta = 0.01$, $\phi = 0.2$.

3.3 Dimensionless Response time:

The graph shown in figure 12 is the variation in time T^* with respect to h_1^* for various C values for permeability parameter $\psi = 0.001$. It is observed that for higher C values the squeezing time T^* is greater for azimuthal structure where as reduces for radial roughness parameter. The

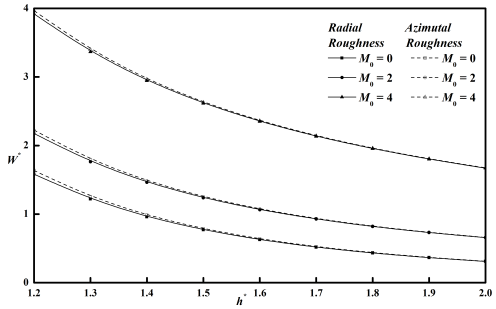

Figure 8: Variation of non-dimensional W^* with h^* for different values of M_0 with $l^* = 0.3$, $C = 0.2$, $\theta = \pi/3$, $\psi = 0.001$, $m = 0.6$, $\delta = 0.01$, $\phi = 0.2$.

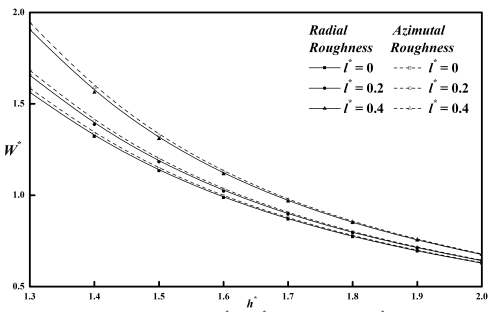

Figure 9: Variation of non-dimensional W^* with h^* for different values of l^* with $M_0 = 2$, $C = 0.2$, $\theta = \pi/3$, $\psi = 0.001$, $m = 0.6$, $\delta = 0.01$, $\phi = 0.2$.

variation of T^* against h_1^* as a function of M_0 for $l^* = 0.3, \theta = \pi/3, C = 0.2$ and $\psi = 0.001$ is shown in figure 13 and found that that the presence of magnetic field enhances squeezing time T^*. In figure 14 the profile T^* against h_1^* as a function of l^* is shown and observed that the impact of couplestress is to enhance T^* as compared to Newtonian fluids for both rough structures. The deviation in time $T^*$with respect to h_1^* for distinct θ values with $M_0 = 2, C = 0.2, l^* = 0.3, \psi = 0.001$ is described in figure 15 and observed that for higher values the time reduces in both structure of roughness. Figure 16 describes the variation in film time T^* against h_1^* for distinct permeability parameter values with $M_0 = 2, C = 0.2, l^* = 0.3, \theta = \pi/3$. It is noted that permeability ψ decreases the squeeze film time for both structure of roughness

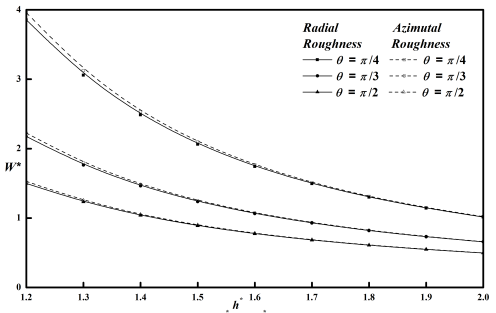

Figure 10: Variation of non-dimensional W^* with h^* for different values of θ with $M_0 = 2$, $C = 0.2$, $l^* = 0.3$, $\psi = 0.001$, $m = 0.6$, $\delta = 0.01$, $\phi = 0.2$.

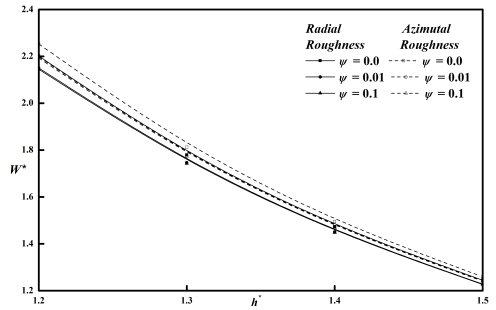

Figure 11: Variation of non-dimensional W^* with h^* for different values of ψ with $M_0 = 2$, $C = 0.2$, $l^* = 0.3$, $\theta = \pi/3$, $m = 0.6$, $\delta = 0.01$, $\phi = 0.2$.

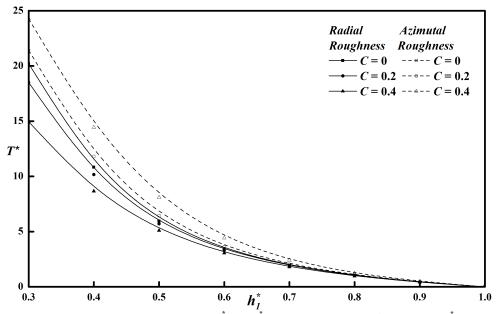

Figure 12: Variation of non-dimensional T^* with h_1^* for different values of C with $M_0 = 2$, $l^* = 0.3$, $\theta = \pi/3$, $\psi = 0.001$, $m = 0.6$, $\delta = 0.01$, $\phi = 0.2$.

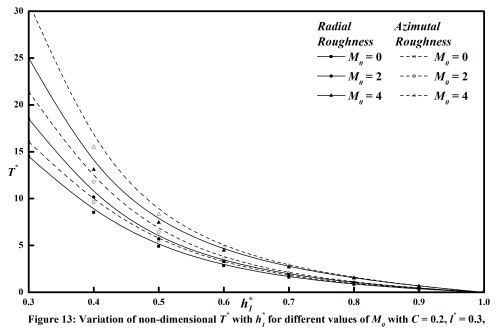

Figure 13: Variation of non-dimensional T^* with h_1^* for different values of M_0 with $C = 0.2$, $l^* = 0.3$, $\theta = \pi/3$, $\psi = 0.001$, $m = 0.6$, $\delta = 0.01$, $\phi = 0.2$.

4 Conclusion

In the present study the characteristic of squeeze film for porous conical plates with CSF and surface roughness in the presence of magnetic field is analysed. From the above result and discussion we can draw following conclusion.

(a). Due to the impact of rough surface ,the pressure , load carrying capacity and time rises for azimuthal structure, than the radial roughness structure. Both the rough structure coincides at $C = 0$.

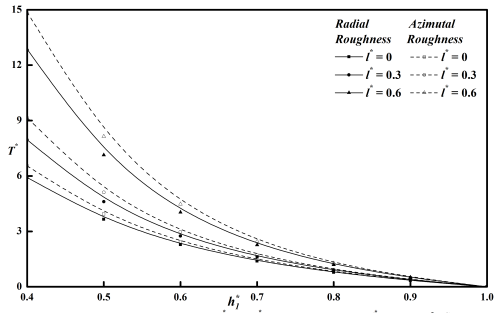

Figure 14: Variation of non-dimensional T^* with h_1^* for different values of l^* with $M_0 = 2$, $C = 0.2$, $\theta = \pi/3$, $\psi = 0.001$, $m = 0.6$, $\delta = 0.01$, $\phi = 0.2$.

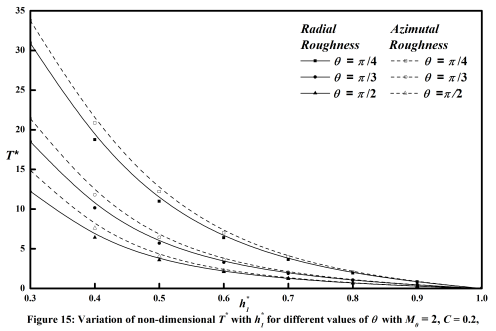

Figure 15: Variation of non-dimensional T^* with h_1^* for different values of θ with $M_0 = 2$, $C = 0.2$, $l^* = 0.3$, $\psi = 0.001$, $m = 0.6$, $\delta = 0.01$, $\phi = 0.2$.

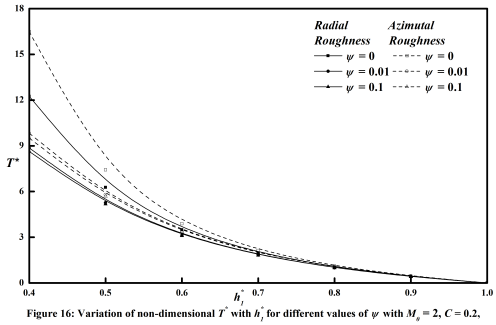

Figure 16: Variation of non-dimensional T^* with h_1^* for different values of ψ with $M_0 = 2$, $C = 0.2$, $l^* = 0.3$, $\theta = \pi/3$, $m = 0.6$, $\delta = 0.01$, $\phi = 0.2$.

(b). With the increase in Hartmann number M_0, the performance of squeeze film improves than compared to the non-magnetic case for radial and film azimuthal structure.

(c). The attributes of squeeze film enhances with the impact of couple stress compared to Newtonian fluids for both the roughness pattern.

(d). For both the rough structure, the pressure, load and squeezing time decreases, with increasing half-cone angle.

(e). The effect permeability parameter reduces the overall performance of squeeze film attributes for both the roughness parameter.

Table:1 A numerical comparison of the present paper with Hanumagowda.et.al[8] is shown in the below table

		Hanumagowda et. al.		Current Analysis					
				C=0 ψ=0		C=0.2, ψ=0.001		C=0.2, ψ=0.01	
	M_0	l^*=0.2	l^*=0.4	l^*=0.2	l^*=0.4	l^*=0.2		l^*=0.2	
						Radial	Azimuthal	Radial	Azimuthal
W^*	M_0=0	14.7525	26.6505	14.7525	26.6505	12.3125	13.8399	5.84	5.9851
	M_0=2	15.9295		15.9295	27.8322	14.119	15.901	13.143	14.5379
	M_0=4	19.4563	31.3759	19.4563	31.3759	18.2032	20.1279	18.005	19.8585
	M_0=6	25.3203	37.2776	25.3203	37.2776	24.3333	26.2589	24.2511	26.1548
T^*	M_0=0	2.58724	4.14293	2.58724	4.14293	2.32652	2.53007	1.45803	1.50214
	M_0=2	2.94694	4.50467	2.94694	4.50467	2.74946	2.96726	2.63693	2.82314
	M_0=4	4.02268	5.58862	4.02268	5.58862	3.8787	4.09922	3.85314	4.06818
	M_0=6	5.80523	7.39116	5.80523	7.39116	5.67886	5.89904	5.6664	5.88507

References

[1] E. A. Hazma, The Magnetohydrodynamic squeeze film, Journal of Tribology. 110 (1988) 375-377 *Math. Scand.* **1, 39–54 (1953).**

[2] J. R. Lin, Magneto-hydrodynamic squeeze film characteristics for finite rectangular plates. Industrial Lubrication and Tribology.55(2) (2003) 84-89.

[3] V. K.Stokes, Couple stresses in fluids, Physics of fluids. 9 (1966) 1709 -1715.

[4] J.R. Lin, Squeeze film characteristics between a sphere and a flat plate: couple stress fluid model, Computers and Structures. 75(2000) 73-80.

[5] N. B. Naduvinamani, Syeda Tasneem Fathima and B. N. Hanumagowda, Magneto-Hydrodynamic couplestress Squeeze film lubrication of Circular Stepped Plates, Journal of Engineering Tribology. 225 (2010) 111-119.

[6] N. B. Naduvinamani and M. Rajashekar, MHD Couplestress Squeeze Film Characteristics between Sphere and Plane Surface, Tribol. – MSI. 5(3) (2011) 94-99.

[7] Syeda Tasneem Fathima, N. B. Naduvinamani, B. N. Hanumagowda and J. K. Santhosh Kumar, Modified Reynolds equation for different types of finite plates with the combined effect of MHD and couplestresses, Tribology Transactions. 58 (2015) 660 - 667.

[8] B. N. Hanumagowda, Swapna .S. Nair and M. Vishu Kumar, Effect of MHD and Couple Stress on Conical Bearing, IJPAM. 113(6) (2017) 316-324.

[9] B. N. Hanumagowda, A. Salma, B.T. Raju and C. S. Nagarajappa, The Magneto-hydrodynamic Lubrication of Curved Circular Plates With Couple Stress Fluid, IJPAM. 113(6) (2017) 307-315..

[10] Morgan, V. T. and Cameron, A., "Mechanism of lubrication in porous metal bearings," In Proceedings of the Conference on Lubrication and Wear, Institution of Mechanical Engineers, London, (1957)151-157.

[11] Rouleau, W. T., "Hydrodynamic lubrication of narrow press-fitted porous metal bearings," Journal of Basic Engineering, 85: (1), (1963) 123-128.

[12] Wu, Hai., "Squeeze-film behaviour for porous annular disks," Journal of Lubrication Technology, 92(4): (1970) 593-596.

[13] Cusano, C. "Lubrication of porous journal bearings," Journal of Lubrication Technology 94(1):(1972): 69-73.

[14] Prakash, J. and Vij, S. K., "Hydrodynamic lubrication of a porous slider," Journal of Mechanical Engineering Science, 15 (3):(1973) 232-234.

[15] Tian, Yong., "Static study of the porous bearings by the simplified finite element analysis," Wear, 218(2) (1998) 203-209.

[16] Christensen, H., "Stochastic model for hydrodynamic lubrication of rough surfaces," Proceedings of the Institution of Mechanical Engineers, 184: (1970):1013-1026.

[17] Prakash, J. and Tiwari, K., "Effect of surface roughness on the squeeze film between rotating porous annular discs," Journal of Mechanical Engineering Science, 24 (3):(1982):155-161.

[18] Gururajan, K. and Prakash, J., "Effect of surface roughness in a narrow porous journal bearing," Journal of Tribology, 122(2) :(2000) :472-475.

[19] Bujurke, N. M. and Kudenatti, R. B., "MHD lubrication flow between rough rectangular plates," Fluid Dynamics Research, 39(4) :(2007): 334-345.

[20] Syeda Tasneem Fathima, Naduvinamani, N. B., Shivakumar, H. M., Hanumagowda B. N., "A Study on the Performance of Hydromagnetic Squeeze film between Anisotropic Rectangular Plates with Couplestress Fluids," Tribology Online, 9:(2014):1-9.

[21] Biradar, K. and Hanumagowda, B. N., "MHD Effects on Porous Wide Composite Slider Bearings Lubricated with a Couplestress Fluids," Tribology Online. 10(1): 2015):11-20.

[22] Hanumagowda, B. N. Swapna S. N. and Asha, B. S. "Analysis of effect of magneto-hydrodynamic, couple-stress and roughness on conical bearing," JPCS, 1000:(2018)

[23] Hanumagowda, B. N., Tesymol Cyriac, Kavitha, L. and Salma, A., "Analysis of Effect of magneto hydrodynamics and couple stress of steady and dynamic characteristics for porous secant slider bearings," JPCS, 1000, 2018.

[24] Naduvinamani, N. B. and Hosmani, S. S., "Porous exponential slider bearings lubricated with MHD-couple stress fluid," Industrial Lubrication and Tribology, 70(5) :(2018):838-845.

[25] Hanumagowda, B. N., Swapna S. N. and Salma A., "Effect of couple-stress fluid and MHD on porous conical bearing," IJMPERD, 10(3) :(2020) : 8665-8676.

Author information

Hanumagowda B N, Department of Mathematics, School of Applied Sciences, REVA University, Bangalore-560064, Karnataka, India.

Salma A, Department of Mathematics, School of Applied Sciences, REVA University, Bangalore-560064, Karnataka, India.

Swapna S Nair, Department of Management and Commerce, Amity University, Dubai, UAE.
E-mail: hbn123@rediffmail.com

Received: Dec 15 2020.
Accepted: Feb 20 2021.